Emergence of homeostatic epithelial packing and stress dissipation through divisions oriented along the long cell axis

Tom P. J. Wyatt[a,b,c], Andrew R. Harris[c,d,1], Maxine Lam[b,1], Qian Cheng[e], Julien Bellis[b,f], Andrea Dimitracopoulos[a,b], Alexandre J. Kabla[e], Guillaume T. Charras[c,g,h,2,3], and Buzz Baum[b,h,2,3]

[a]Center for Mathematics, Physics, and Engineering in the Life Sciences and Experimental Biology, [b]Medical Research Council's Laboratory for Molecular Cell Biology, [g]Department of Cell and Developmental Biology, and [h]Institute for the Physics of Living Systems, University College London, London WC1E 6BT, United Kingdom; [c]London Centre for Nanotechnology, University College London, London, WC1H 0AH, United Kingdom; [d]Bioengineering, University of California, Berkeley, CA 94720; [e]Department of Engineering, University of Cambridge, Cambridge CB2 1PZ, United Kingdom; and [f]Centre de Recherche de Biochimie Macromoléculaire, 34293 Montpellier, France

Edited by David A. Weitz, Harvard University, Cambridge, MA, and approved March 31, 2015 (received for review November 3, 2014)

Cell division plays an important role in animal tissue morphogenesis, which depends, critically, on the orientation of divisions. In isolated adherent cells, the orientation of mitotic spindles is sensitive to interphase cell shape and the direction of extrinsic mechanical forces. In epithelia, the relative importance of these two factors is challenging to assess. To do this, we used suspended monolayers devoid of ECM, where divisions become oriented following a stretch, allowing the regulation and function of epithelial division orientation in stress relaxation to be characterized. Using this system, we found that divisions align better with the long, interphase cell axis than with the monolayer stress axis. Nevertheless, because the application of stretch induces a global realignment of interphase long axes along the direction of extension, this is sufficient to bias the orientation of divisions in the direction of stretch. Each division redistributes the mother cell mass along the axis of division. Thus, the global bias in division orientation enables cells to act collectively to redistribute mass along the axis of stretch, helping to return the monolayer to its resting state. Further, this behavior could be quantitatively reproduced using a model designed to assess the impact of autonomous changes in mitotic cell mechanics within a stretched monolayer. In summary, the propensity of cells to divide along their long axis preserves epithelial homeostasis by facilitating both stress relaxation and isotropic growth without the need for cells to read or transduce mechanical signals.

morphogenesis | cell division | mechanical feedback | quantitative biology | mitotic rounding

The morphogenesis of animal tissues results from coordinated changes in the shape, size, and packing of their constituent cells (1–3). These include autonomous cell shape changes (4), the response of cells to extrinsic stresses, and the effects of passive tissue deformation (5). When coordinated across a tissue, these active cellular processes and passive responses enable epithelial sheets to undergo shape changes while retaining relatively normal cell packing (6) and help return tissues to their resting state following a perturbation (7). Although the molecular basis of this cooperation is not understood, several studies have suggested a role for mechanical feedback (8, 9). Cell division has been suggested to participate in this feedback (10) because the rate of animal cell proliferation responds to changes in extrinsic forces in several experimental settings (9). Further, division makes an important contribution to tissue morphogenesis in animals (11, 12), accounts for much of the topological disorder observed in epithelia (13), can drive tissue elongation (10), and can facilitate the return to homeostatic cell packing following a deformation (2). Importantly, for each of these functions, the impact of cell division depends critically on the orientation of divisions.

At the cellular level, relatively simple rules appear to govern division orientation. These rules were first explored by Hertwig (14), who showed that cells from early embryos divide along their long axis, and were further refined using microfabricated chambers (15). However, by following division orientation in cells adhering to micropatterned substrates, more recent studies identified additional roles for both the geometrical arrangement of integrin-mediated cell–substrate adhesions (16) and extrinsic mechanical forces in orienting divisions (17). Consistent with this, adhesive and mechanical cues have been reported to guide division orientation in vivo (18) and in epithelial monolayers in developing embryos (12, 19). Nevertheless, the respective roles of cell shape and mechanical tension in guiding division orientation in epithelia remain poorly defined, as does the contribution of oriented division to mechanical feedback control.

Previously, we established suspended epithelial monolayers lacking ECM as a minimal model system in which to study epithelial biology. Because cell divisions in these monolayers become oriented following a stretch, we were able to explore the regulation and function of division orientation. We found that divisions align better with the long, interphase cell axis than with the monolayer stress axis. This phenomenon, combined with the alignment of cellular long axes induced by stretch, results in a global bias in the orientation of divisions in the direction of extension. Each division

Significance

Animal cells undergo a remarkable series of shape changes as they pass through mitosis and divide. In an epithelial tissue, the impact of these morphogenetic processes depends strongly on the orientation of division. However, the cues orienting divisions remain poorly understood. Here, we combine live imaging and mechanical perturbations with computational modeling to investigate the effects of shape changes accompanying mitosis and division in stretched monolayers in the absence of neighbor exchange. We show that divisions orient with the long cell axis rather than with the stress direction, and show how oriented divisions contribute to the restoration of cell packing and stress relaxation. In doing so, we identify a clear role for oriented cell division in morphogenetically active tissues.

Author contributions: T.P.J.W., A.J.K., G.T.C., and B.B. designed research; T.P.J.W., A.R.H., Q.C., and J.B. performed research; T.P.J.W., M.L., Q.C., J.B., and A.D. analyzed data; and T.P.J.W., A.J.K., G.T.C., and B.B. wrote the paper.

The authors declare no conflict of interest.

This article is a PNAS Direct Submission.

[1]A.R.H. and M.L. contributed equally to this work.

[2]G.T.C. and B.B. contributed equally to this work.

[3]To whom correspondence may be addressed. Email: g.charras@ucl.ac.uk or b.baum@ucl.ac.uk.

This article contains supporting information online at www.pnas.org/lookup/suppl/doi:10.1073/pnas.1420585112/-/DCSupplemental.

redistributes cell mass along the axis of division. Thus, when oriented across a monolayer, divisions act collectively to redistribute mass along the axis of stretch, helping to return the monolayer to its resting state. In summary, this analysis shows that the propensity of cells to divide along their long axis preserves epithelial homeostasis by facilitating both stress relaxation and isotropic growth without the need for cells to read or transduce mechanical signals.

Results

Uniaxial Monolayer Extension Results in Sustained Cell Elongation and Tension Oriented Along the Axis of Stretch. Previously, we used suspended Madin–Darby canine kidney II (MDCK) monolayers as a model system with which to study epithelial mechanics (20). For the study of cell division in monolayers, we modified the device (21) to allow imaging over several hours (Fig. S1). Following a stretch, cells in suspended monolayers did not change neighbors (Fig. S2). Instead, they responded by elongating in the direction of stretch by an amount roughly equal to the amount applied at the monolayer level (20). Extension was accompanied by a decrease in monolayer thickness (20) and a small decrease in width. Cells then remained elongated until they divided (Fig. 1 *A* and *B* and Fig. S3).

We confirmed that suspended monolayers generated through collagenase treatment (20) were devoid of a continuous load-bearing ECM but retained apicobasal polarization over the course of our experiments (Fig. S4). Hence, the transmission of tension across suspended monolayers depends entirely on intercellular junctions, which remained stable over the duration of our experiments. To estimate the tension borne by individual cells following stretch, we monitored monolayer tension over 200 min. Tension was maximal immediately after deformation before decreasing by 75% within 2 min (Fig. 1*C*). This initial relaxation was followed by a slower but steady decrease in tension, which remained at ∼40 nN per cell for the duration of these experiments (Fig. 1*D*). When the mechanical integrity of individual cells was perturbed using a pulsed 405-nm laser, we observed local recoil as expected for a tissue under tension. We then analyzed the orientation of this mechanical recoil to determine the orientation of stresses at the cellular scale (Fig. 1 *E* and *F* and Fig. S5). In all cases, the local stress field was closely aligned with the axis of stretch, regardless of the orientation of the long axis of the targeted cell (Fig. 1*F*).

Taken together, these data show that a 30–35% monolayer extension induces a significant change in cell shape and orientation, resulting in an average cell aspect ratio of ∼1.4, with 55% of cells oriented within 20° of the stretch axis (Fig. 1*B*). Cells within stretched monolayers were exposed to a sustained local stress that was closely aligned with the extension axis. This resulted in a tension of ∼40 nN per cell, which is several-fold larger than necessary to orient division in adherent cells (17). Thus, cells in stretched monolayers are both elongated and subjected to significant tension, both of which are known to orient cell divisions. Suspended monolayers therefore constitute an ideal system in which to explore the relative importance of force and shape in the orientation of cell division.

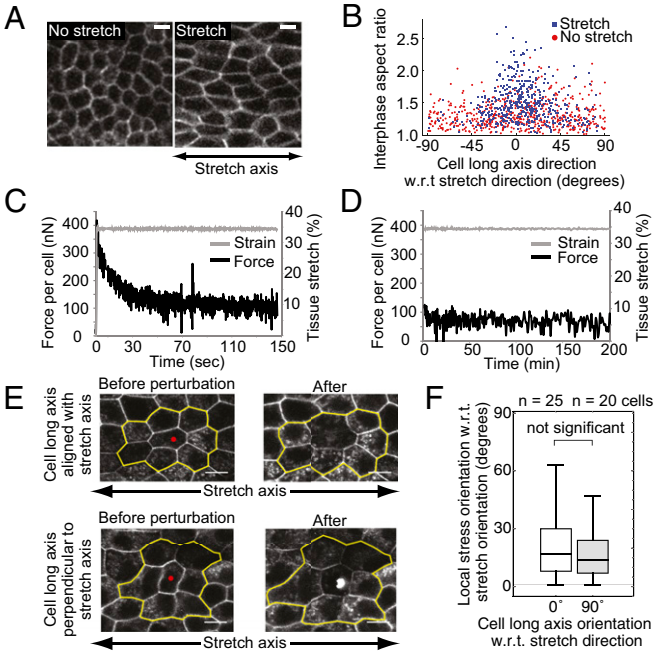

Fig. 1. Uniaxial stretch results in long-term cellular elongation and monolayer stress. (*A*) Monolayers expressing E-cadherin–GFP before and after a 30% stretch. (Scale bars: 10 μm.) (*B*) Orientation and aspect ratio of cells in stretched (blue) and nonstretched (red) monolayers, as calculated from the orientation and major-to-minor axis ratio of the best-fit ellipse to the cell shape. w.r.t., with respect to. The evolution of strain (gray) and force (black) in a stretched monolayer for short (*C*, up to 150 s) and long (*D*, up to 200 min) time scales is shown. (*E*) Cells expressing E-cadherin–GFP in a stretched monolayer before and after perturbation of their mechanical integrity by a pulsed-UV laser. Cells with shapes oriented ∼0° (*Top*) and ∼90° (*Bottom*) to the direction of stretch were chosen. Red dots indicate the area where the laser was applied. Yellow outlines mark the region including the nearest neighbors of the perturbed cell. (Scale bars: 10 μm.) (*F*) Local orientation of stress, as measured from recoil after laser perturbation, for cells with shapes oriented ∼0° and ∼90° to the stretch direction. The horizontal line and top and bottom of boxes represent the median, 75th percentile, and 25th percentile in all box plots, respectively. The whiskers demarcate the range ($n \geq 20$ cells and $n \geq 12$ monolayers for each condition).

Effect of Stretch on Cell Division in Suspended Monolayers. Mitotic progression within suspended monolayers was visualized using E-cadherin–GFP (Fig. 2*A* and Movie S1). We first explored the timing of divisions. A transient inhibition of mitotic entry was observed following stretch (Fig. S6*A*); however, mitosis resumed some 60 min later. Interestingly, the cells that entered mitosis after this transient delay tended to be those with the largest apical area (Fig. S6 *B* and *C*) rather than the most elongated, as would have been expected if mitotic entry were triggered by a mechanical cue. These cells then all divided in the plane of the epithelium, as observed for monolayers growing on substrates (22) (Fig. 2*A* and Fig. S7). Whereas cells in nonstretched monolayers divided with no orientational bias (Fig. 2*B*), a 30–35% strain was sufficient to induce a global bias in the orientation of divisions (Fig. 2*B*), such that 56% of cells divided within 20° of the stretch axis.

Although previous work has implicated mechanical forces in orienting epithelial cell divisions (19), determining the relative importance of interphase shape and tension is challenging. To do so, we compared the orientation of the stretch axis, the interphase long cell axis, and the division axis in the presence and absence of stretch. Cells with a well-defined interphase long cell axis (measured as an aspect ratio, $r > 1.4$) reliably divided along so axis in both stretched and nonstretched monolayers, with 82 ± 2% and 77 ± 4% of divisions, respectively, occurring within 20° of the interphase long cell axis (Fig. 2*C*). Moreover, mitotic cells were polarized in both stretched and nonstretched monolayers, with their spindles aligned with the long cell axis and with known cortical regulators of spindle orientation concentrated at either pole (Fig. S8). To better separate the influence of tension from the influence of cell shape, we examined the small subset (∼5%) of elongated cells whose interphase long axis was misoriented (>35°) with respect to the axis of stretch [Fig. 2 *C* (red points), *D*, and *E* (red points) and Fig. S3*C*]. Strikingly, when these cells divided, their divisions were always better aligned with the interphase long cell axis than with the axis of applied stretch (Fig. 2*E*). This was the case despite these cells being subjected to significant local forces aligned along the global stretch axis (Fig. 1 *E* and *F*). Taken together, these data suggest that the alignment of divisions across a stretched monolayer is the simple result of a stretch-induced global bias in the orientation of long cell axes combined with the propensity of cells to divide along their long axis.

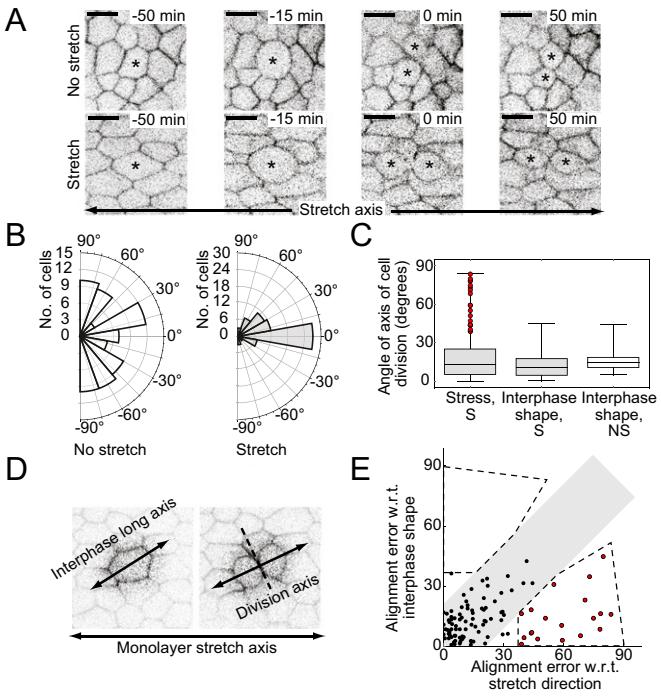

Fig. 2. Divisions align along the interphase long cell axis monolayers. (*A*) Time series of a dividing cell expressing E-cadherin–GFP to enable visualization of intercellular junctions in a nonstretched monolayer and a stretched monolayer. Time is measured from division. Asterisks mark dividing and daughter cells. (Scale bars: 10 μm.) (*B*) Orientation of division with respect to the direction of stretch or with respect to the direction perpendicular to the test rods in the no-stretch case ($n \geq 72$ divisions and $n = 3$ monolayers for each condition). (*C*) Orientation of division with respect to the axis of stretch (stress, *Left*), to the interphase shape orientation in stretched monolayers (*Middle*), and to the interphase orientation in nonstretched monolayers (*Right*) for elongated cells ($r > 1.4$). Cells marked by a red point correspond to those appearing in red in *E*. NS, nonstretched; S, stretched. (*D*) Dividing cell in a stretched monolayer. The interphase shape is misaligned with the direction of monolayer stress, and the division follows the interphase shape rather than the monolayer stress direction. (*E*) Error in alignment of division with the monolayer stress axes plotted against the error in alignment with interphase shape for elongated ($r > 1.4$) cells in stretched monolayers. The gray shading shows the region in which divisions align equally well with monolayer stress and interphase shape. Dotted lines demarcate regions where divisions align significantly better with interphase shape than stress, and vice versa.

Effect of Monolayer Stress on Mitotic Rounding. Next, we investigated the morphological changes accompanying passage through mitosis in cells to assess if changes following a stretch might aid monolayer relaxation (Fig. 2*A* and Movie S1). Within nonstretched monolayers, cells entering mitosis assumed a near-isotropic metaphase shape in the plane of the epithelium (aspect ratio, $r_{-\text{stretch}} = 1.16 \pm 0.02$; Figs. 2*A* and 3*A*), as do most primary cells and cell lines cultured on ECM (23). By contrast, cells within stretched monolayers were unable to round fully before division (aspect ratio, $r_{+\text{stretch}} = 1.25 \pm 0.02$; Figs. 2*A* and 3*A*), despite a shortening in their interphase long axis that was larger than observed in nonstretched monolayers (Fig. 3*B*). In vitro measurements show that individual cells generate a rounding force of ∼80 nN upon entry into mitosis (24). Therefore, the failure of cells to round completely in stretched monolayers is likely a simple consequence of residual monolayer tension (∼40 nN per cell; Fig. 1*D*).

When we measured the evolution of cell dimensions parallel and perpendicular to the axis of division at 5-min intervals, we found clear differences between cells in nonstretched and stretched monolayers. Cells within nonstretched monolayers retained a roughly constant aspect ratio until anaphase, when it increased sharply (Fig. 3 *D*, *ii*). At abscission, the aspect ratio was halved and remained constant over the following 60 min (Fig. 3 *D*, *iii*). This behavior contrasted with the behavior of cells within stretched monolayers, which displayed a marked decrease in aspect ratio upon entry into mitosis (Fig. 3 *D*, *i*), reflecting their more elongated initial shape. Cellular aspect ratio then increased sharply at anaphase before being halved following abscission (Fig. 3 *D*, *ii*). Then, in contrast to cells in nonstretched monolayers,

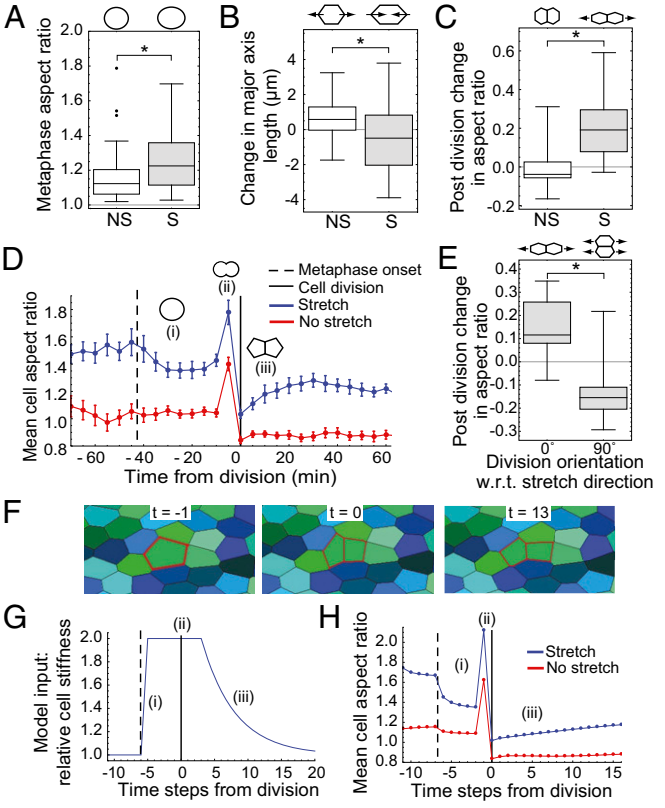

Fig. 3. Effect of monolayer stress on mitotic rounding. (*A*) Box-whisker plots showing the metaphase aspect ratio of dividing cells in nonstretched and stretched monolayers (*$P < 0.002$). (*Top*) Diagrams show the median shape of rounded cells in each condition. (*B*) Changes in the long cell axis length during rounding in nonstretched and stretched monolayers. (*Top*) Diagrams show the most frequent direction of shape change during rounding in each condition ($n \geq 48$ cells and $n = 3$ monolayers for each condition; *$P < 0.001$). (*C*) Change in cell aspect ratio (measured with respect to the direction of division) between division ($t = 0$) and $t = 25$ min ($n = 20$ cells for each condition; *$P < 0.001$). (*D*) Temporal evolution of the mean cell aspect ratio (measured with respect to the direction of division) of dividing cells. Data points are averaged over $n = 10$ cells in both stretched (blue) and nonstretched (red) monolayers. Division was taken as time 0 (solid vertical line). Rounding onset (dashed line), anaphase, and daughter cell reintegration are marked by (*i*), (*ii*), and (*iii*), respectively, and are represented by pictograms. From time 0 onward, the values represent the average over all individual daughter cells. Error bars indicate SE. (*E*) Change in cell aspect ratio (measured with respect to the direction of division) between division ($t = 0$) and $t = 25$ min for cells without a well-defined long axis ($r < 1.25$) in stretched monolayers ($n \geq 18$ cells were characterized for each condition; *$P < 0.001$). (*F*) Example time series of division in a computer simulation of a stretched monolayer. The dividing cell and its daughters are highlighted with red junctions. (*G*) Temporal evolution of cell stiffness during mitosis imposed on all dividing cells in simulations. The times marked with (*i*), (*ii*), and (*iii*) correspond to the times described in *D*. (*H*) Temporal evolution of the mean cell aspect ratio for cells in stretched (blue) and nonstretched (red) monolayers in numerical simulations. Times marked with (*i*), (*ii*), and (*iii*) correspond to the times described in *C*. The SE is <0.02, and so is not shown. Each data point represents $n \geq 180$ divisions.

daughter cells in stretched monolayers underwent a gradual increase in their aspect ratio in the 25 min following abscission (Fig. 3 *C* and *D*, *iii*). Daughter cells elongated along the stretch axis regardless of the orientation of division (Fig. 3*E*), implying that it is caused by the extrinsic tension. Overall, these data indicate that extrinsic tension impedes cell rounding at mitotic onset but promotes elongation of daughter cells following division. Surprisingly, cell elongation at anaphase appeared relatively insensitive to extrinsic tension (Fig. 3 *D*, *ii*).

Balance of Cell-Autonomous and Extrinsic Mechanical Forces Explains Changes in Cell Shape Accompanying Mitotic Progression. To test how the clear differences in morphological changes accompanying mitosis between cells in stretched and nonstretched monolayers (Fig. 3) might arise, we developed a mechanical model that could be used to determine how extrinsic stresses likely influence autonomous shape changes accompanying mitotic progression, the redistribution of cell mass following division, and to assess the likely contribution of oriented divisions to the relaxation of monolayer stress.

Cells in the model are represented by linear elastic domains with uniform stiffness calibrated against experimentally measured values (*SI Materials and Methods*). Stress is balanced by treating the monolayer as a continuous elastic material. Although cells can passively slide past each other in response to shear forces along their junctions, cell–cell friction was set high to prevent such rearrangements in this particular implementation to reflect the lack of neighbor exchange in suspended monolayers (Fig. S2). Using these assumptions, simulations computed the new monolayer-scale mechanical equilibrium at each time point during division (Fig. 3*F*). The cell-autonomous changes in cell stiffness (represented by a shear modulus G) used to simulate changes in cortical tension accompanying passage through mitosis were derived from measurements in isolated cells (23, 24). A change in cortical (surface) tension ($\Delta\Gamma$) is related to a change in effective shear modulus (ΔG) by $\Delta G = \Delta\Gamma/R$ (where R is the cell radius) (25). To model mitotic progression, we increased stiffness abruptly at mitotic entry (Fig. 3*G*) and kept it constant until division, before gradually returning it to interphase levels. At division, cells were forced to divide along their interphase long axis.

Strikingly, although these simulations introduced experimentally measured changes in the mechanics of isolated mitotic cells into a model epithelium, they yielded changes in the aspect ratios of cells that were qualitatively and quantitatively similar to those observed in suspended monolayers. Thus, in simulations, the sharp increase in stiffness accompanying entry into mitosis drove complete rounding in control monolayers but only partial rounding in stretched monolayers (Fig. 3 *H*, *i*). In addition, although daughter cells in nonstretched monolayers maintained their shape following division (Fig. 3 *H*, *iii*), they gradually elongated in the direction of applied stress in stretched monolayers, concomitant with the return of stiffness to interphase values (Fig. 3 *H*, *iii* and *G*, *iii*). This finding suggests that experimentally observed changes in cell shape during division are the simple consequence of well-understood autonomous changes in mitotic cell mechanics, removing the need to invoke additional mechanisms.

Cell Division Leads to a Global Redistribution of Mass Within the Monolayer. Next, we investigated the impact of individual cell divisions on local monolayer organization to determine if oriented divisions reduce monolayer stress and/or restore cell packing, as previously proposed (19, 26). We examined changes in the shape of dividing cells as well as changes in the organization of surrounding cells at set time points during mitotic progression reflecting passage from late G2 into mitosis ($t = -60$ and $t = -50$), division ($t = 0$), and reintegration into the epithelium ($t = 50$ and $t = 60$) (diagrams in Fig. 4 *A* and *B*). This analysis indicated that the net effect of division in both stretched and nonstretched monolayers is to redistribute cell mass along the division axis (Fig. 4 *A* and *B*; compare 50–60 min before and after division). At division, the combined daughter cell length was larger than the mother cell length in late G2 by 35 ± 3% in stretched monolayers and 37 ± 4% in nonstretched monolayers (Fig. 4*A*). At 50–60 min after division, combined daughter cell lengths had contracted a little but remained significantly longer than mother cell lengths before division (by 21 ± 3% in stretched monolayers and 18 ± 3% in nonstretched monolayers; Fig. 4*A*). Because width decreased significantly (Fig. 4*B*), the overall effect of division was a significant increase in the aspect ratio of the combined daughter cells compared with their mothers (+41 ± 5% in stretched monolayers and +42 ± 5% in nonstretched monolayers; $P < 0.01$). Qualitatively and quantitatively, similar changes in aspect ratio were obtained from simulations, with an increase of 29% in stretched monolayers and 34% in nonstretched monolayers. Thus, individual divisions lead to the redistribution of mother cell mass along the interphase long axis whether or not the monolayer is under tension.

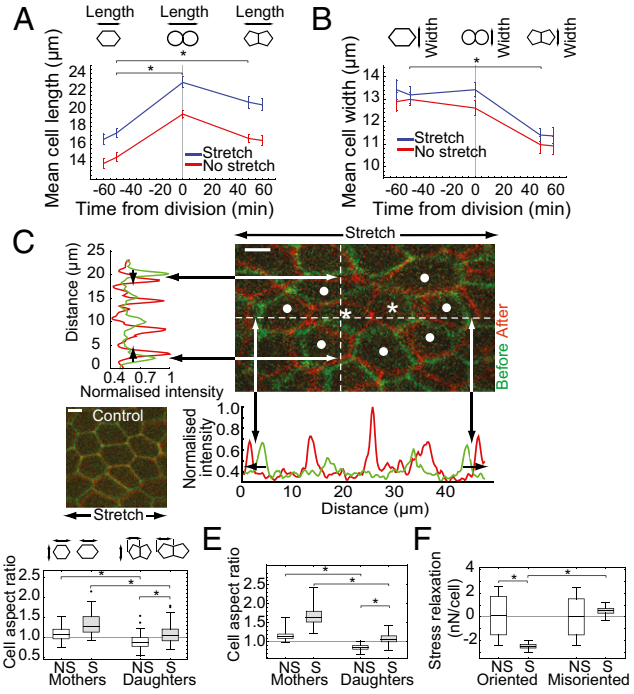

Fig. 4. Effects of stress-induced oriented division on local cell packing and monolayer stress. Temporal evolution of mean cell length (*A*) and mean cell width (*B*) of the mother cell (before division) and of the combined spatial envelope of the daughters (after division) in stretched (blue) and nonstretched (red) monolayers showing mass redistribution in the direction of division. (*Top*) Diagrams depict the measurements taken. Asterisks denote a significant difference between medians (*$P < 0.01$; $n \geq 38$ cells from $n = 3$ monolayers for each condition). Error bars denote SE. (*C*) Overlays of mitotic cells 10 min before (green) and 30 min after (red) furrowing onset. Asterisks mark daughter cells, and dots mark first neighbors. Fluorescence intensity line profiles taken along the dotted lines show shifts in the position of junctions in cells neighboring the dividing cell (black arrows in the fluorescence profile). Junctions shift away from the dividing cell along the axis of division (*Bottom Right*) and toward it in the direction perpendicular to division (*Upper Left*). (*Bottom Left*) No such shifts were observed in overlays of areas containing no division. (Scale bars: 10 μm.) (*D*) Aspect ratio (measured with respect to the direction of division) of stretched and nonstretched cells at 50 min before division (mothers) and 50 min after division (individual daughters) ($n \geq 35$ cells and $n = 3$ monolayers for each condition). (*Top*) Diagrams depict measurement taken. Asterisks denote a significant difference between medians (*$P < 0.01$). (*E*) Same as *D*, but in simulated monolayers ($n \geq 180$ divisions). (*F*) Change in monolayer stress caused by simulated divisions in stretched and nonstretched monolayers in cases where the division is oriented with the cell shape orientation (oriented) or 90° from it (misoriented) ($n \geq 180$ divisions were examined).

To determine the effect of division on local epithelial organization, we compared the position of intercellular junctions close to dividing cells before (green, Fig. 4*C*) and after (red, Fig. 4*C*) division. Division caused an inward movement of neighboring junctions in the direction perpendicular to division, together with an outward movement in the direction of division (Fig. 4*C*). Similar patterns of junctional movement were observed in both stretched and nonstretched conditions ($n = 18$) but were absent in control areas of the monolayer, where divisions did not occur (Fig. 4*C*, *Inset* and Fig. S9). In summary, each division redistributes mass, which leads to local monolayer expansion along the axis of division and contraction in the perpendicular direction. Because there is a global bias in division orientation in stretched monolayers, individual cell divisions act together to expand the monolayer in the direction of stretch and to contract it in the perpendicular direction, leading to an overall effect similar to convergent extension.

Effect of Monolayer Stretch on the Orientation of Subsequent Divisions. To explore how mass redistribution might function over the course of multiple divisions, we then compared the aspect ratio of daughter cells with the aspect ratio of their mothers (Fig. 4*D*). In nonstretched monolayers, mother cells with an average aspect ratio of $\rho = 1.09 \pm 0.03$ divided to generate daughter cells with an aspect ratio of $\rho = 0.91 \pm 0.02$ (Fig. 4*D*). Thus, the long axes of mother and daughter cells tend to be perpendicular to one another. By contrast, in stretched monolayers, mother cells ($\rho = 1.34 \pm 0.05$) gave rise to daughters that remained elongated in the same direction ($\rho = 1.10 \pm 0.03$; Fig. 4*D*). Hence, although division redistributes mass along the division axis in both conditions, the orientation of daughter cells relative to their mothers was altered by stretch. Assuming homogeneous cell growth throughout the monolayer, the second round of divisions will tend to be oriented with the first round in stretched monolayers but perpendicular to the first round in nonstretched monolayers.

Qualitatively and quantitatively, similar results were obtained in the model (Fig. 4*E*). In stretched monolayers, daughter cells retained the same orientation as their mothers ($\rho = 1.03 \pm 0.03$), whereas in nonstretched monolayers, they tended to be oriented perpendicular to the mother cell ($\rho = 0.84 \pm 0.03$). Finally, because the model faithfully replicates the observed cell shape changes accompanying mitosis, we were able to use it to predict the impact of divisions on monolayer stress. In nonstretched monolayers, division had no net effect on monolayer stress (Fig. 4*F*), as expected under conditions of isotropic monolayer growth. Conversely, in stretched monolayers, divisions along the cellular long axis dissipated monolayer stress, whereas divisions perpendicular to it did not (Fig. 4*F*). Taken together, these data show how isotropic monolayer growth and the restoration of homeostasis following a stretch can both be understood as emergent properties resulting from the simple ability of cells to orient their division along their interphase long axis.

Discussion

Although it is widely accepted that animal tissues are mechanosensitive (9), the physical parameters that cells respond to have yet to be defined. This is true even for instances in which an applied force is known to induce a well-defined cellular response. One of the most biologically significant examples of this is oriented cell division, a process that plays a key role in tissue morphogenesis (27) and tissue relaxation (19). However, many aspects of the process remain unclear. For example, it is not known how tissue stress affects the morphological changes accompanying cell division. In addition, because the application of force tends to induce both stress and strain, it is challenging to determine the extent to which divisions orient in response to tension and/or cellular deformation. Finally, it is unclear how individual oriented divisions contribute to stress relaxation and tissue homeostasis.

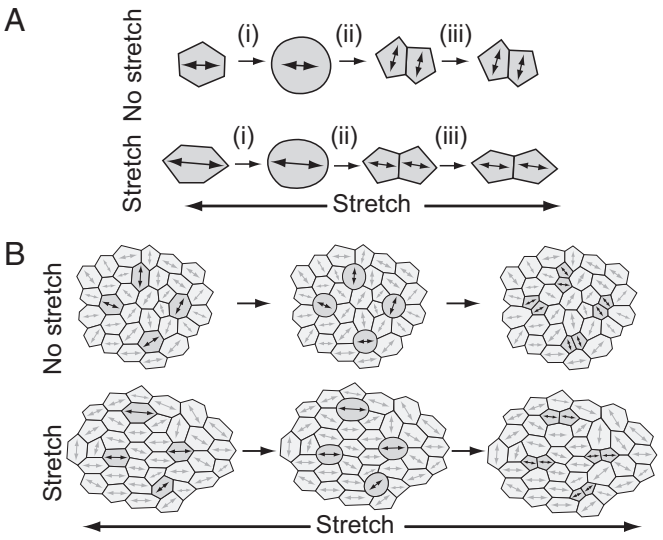

Fig. 5. Epithelial monolayer homeostasis is an emergent property of cell division oriented along the interphase long cell axis. (*A*) Diagram depicting the behavior of individual cells undergoing division along their long axis in nonstretched and stretched monolayers. Mother cells in stretched monolayers are initially more elongated and fail to round to same extent as cells in the nonstretched control. In both stretched and nonstretched cells, the division orients with cell interphase shape. In nonstretched cells, the division creates daughter cells that are oriented approximately orthogonal to the orientation of the mother cell, and there is little or no change in shape afterward. The division in stretched cells creates daughter cells oriented along the same axis as the mother cell. Immediately after abscission, daughter cells are approximately isotropic, but they then elongate over the following ~25 min. The arrows marked with (*i*), (*ii*), and (*iii*) correspond to rounding onset, anaphase, and daughter cell reintegration, respectively. (*B*) Diagram depicting the effect of the behavior in *A* at the monolayer level. The randomly oriented cell shapes in nonstretched monolayers cause divisions to be oriented with a uniform angular distribution, so there is no net directional effect. In stretched monolayers, the long cell axes are preferentially aligned with the direction of stretch. Preferential division of cells along their long axes therefore results in a global bias in division in this direction, which is likely to be preserved in consecutive divisions.

Here, we used suspended epithelial monolayers as an experimental model to address each of these questions. Several features make suspended monolayers an ideal simplified model. First, in the absence of a continuous substrate, all monolayer-level forces are transmitted across cell–cell junctions. Second, monolayer deformation can be precisely controlled and monolayer-level forces can be accurately measured over time. Third, cells do not change neighbors during the time course of experiments relevant to the study of cell division.

Following a 30–35% strain, cells in suspended monolayers remained elongated by ~30% along the stretch axis and, simultaneously, experienced a sustained, uniformly oriented tension of ~40 nN per cell. This is approximately threefold higher than the tensions found to orient division in isolated adherent cells (17). After transient inhibition of mitotic entry induced by stretch, cells with the largest apical areas entered mitosis before dividing along the stretch axis. These cells were then used to investigate the relative roles of tension and cell shape in orienting divisions, as well as the function of oriented cell division in the restoration of cell packing and force relaxation following a stretch.

To assess whether the division axis is determined by the stress axis, as recently suggested (17, 19), or by cell shape, as suggested by Hertwig (14) and other researchers using nonadherent cells from early embryos (15), we focused our attention on the subset of cells whose interphase long axis was misoriented relative to the tension axis. Strikingly, these cells divided along their interphase long axis (Fig. 2 *C–E*), even though this axis differed

from the local stress axis (Fig. 1 *E* and *F*). Thus, cell geometry dominates over cellular-level stress in the control of division orientation under the experimental conditions tested here. Consistent with this, the polarization of mitotic cortical markers was aligned with the long cell axis in stretched and nonstretched monolayers. Further, the orientation of division along the long cell axis was as accurate in nonstretched monolayers as it was in stretched monolayers. Therefore, in suspended monolayers, it is the change in cell shape induced by monolayer extension that dictates the global bias in spindle orientation. It remains to be determined whether this is also true in other systems and/or is related to the lack of an ECM (16).

How do individual oriented divisions affect monolayer mechanics in our system? In both stretched and nonstretched monolayers, division was accompanied by a marked redistribution of cell mass along the interphase long axis. This mass redistribution appeared to be triggered by the process of anaphase elongation, which lengthened and narrowed the spatial envelope of the two daughter cells relative to the mother cell (Figs. 4 *A* and *B* and 5*A*). This morphogenetic process led to local monolayer expansion along the axis of division and a contraction in the perpendicular direction. Because stretch induces a global reorientation of cellular long axes along the axis of stretch, when summed across the monolayer, mass redistribution is expected to facilitate monolayer relaxation. This conclusion was confirmed by numerical simulations based on cell-autonomous changes in mitotic cell stiffness, making it clear that our observations can be explained without the need to invoke mechanosensory signaling. Moreover, the same simulations showed that division only contributes to global stress dissipation when oriented along the long-cell axis (Fig. 4*F*).

Both the experimental data and the model suggest that, in stretched monolayers, mother and daughters will tend to divide in the same orientation over successive divisions until cell shape becomes isotropic (Figs. 4 *D* and *E* and 5*A*), restoring cell packing. In contrast, the orientation of divisions will tend to alternate in nonstretched monolayers, promoting isotropic monolayer growth, as commonly observed in proliferating plant tissues, where no neighbor exchange occurs (28).

Taken together, these data suggest a model (Fig. 5) in which mechanical tension operating at the monolayer scale causes interphase cells to elongate in the direction of stretch. This elongation biases cell divisions so that they orient along the interphase long axis. Because divisions redistribute mass, this facilitates stress relaxation and the restoration of cell packing over one or more rounds of division in a way that is analogous to passive cell intercalation (29). Thus, stress relaxation in suspended monolayers appears to be an emergent property that arises from the autonomous behavior of individual cells following the same simple rule to divide along their long cell axis.

Materials and Methods

Generation and Imaging of Suspended Monolayers. Suspended monolayers were generated as described by Harris et al. (21). Briefly, stretching devices were built from glass capillaries (Sutter Instruments) and a length of nickel-titanium (nitinol) wire (Euroflex) that acted as a hinge (Fig. S1). Glass coverslips (VWR) on which the cells would grow were glued to the devices. Reconstituted collagen (Cellmatrix) was suspended between the platforms and dehydrated to form a scaffold onto which MDCK cells were seeded. After ~72 h of culture, the collagen was digested and stretch was applied with a manual manipulator. Monolayers were imaged with either an inverted spinning disk (Yokogawa) confocal microscope or an FV-1000 scanning laser confocal microscope (Olympus), both with environmentally controlled enclosures. MDCK cells stably expressing E-cadherin–GFP were used for visualizing cell–cell junctions for live imaging and otherwise were fixed in 4% (wt/vol) PFA before immunostaining. Image analysis was performed in Fiji (ImageJ) or in custom MATLAB (MathWorks) or Mathematica (Wolfram Research, Inc.) scripts. More information is provided in *SI Materials and Methods*.

Mechanical Model. Cell division was implemented in a force-based computational model. A Voronoi tessellation divides the tissue into cells, and forces act on the edges of these polygons. Cells are represented as a strain tensor and interact with other cells through contact force and viscous force. Force balance is applied to each cell to compute the shear forces at cell edges that lead to remodeling. More information is provided in *SI Materials and Methods*.

ACKNOWLEDGMENTS. We thank D. Farquharson and S. Townsend at the University College London workshop and Joel Jennings and Richard Adams for help with model development. B.B. and J.B. thank Cancer Research UK, the Biotechnology and Biological Sciences Research Council (BBSRC) (Grant BB/K009001), the French Institut National du Cancer, and Matthieu Piel for support. T.P.J.W. and A.D. were supported by the Engineering and Physical Sciences Research Council. A.R.H. was supported by the BBSRC (Grant BB/K013521 to G.C. and A.K.), and M.L. was supported by the Agency for Science Technology and Research (Singapore) and the Wellcome Trust.

1. Farge E (2011) Mechanotransduction in development. *Forces and Tension in Development*, ed Labouesse M (Academic, Waltham, MA), 1st Ed, Vol 95, pp 243–265.
2. Gibson WT, et al. (2011) Control of the mitotic cleavage plane by local epithelial topology. *Cell* 144(3):427–438.
3. Bosveld F, et al. (2012) Mechanical control of morphogenesis by Fat/Dachsous/Four-jointed planar cell polarity pathway. *Science* 336(6082):724–727.
4. Martin AC, Kaschube M, Wieschaus EF (2009) Pulsed contractions of an actin-myosin network drive apical constriction. *Nature* 457(7228):495–499.
5. Butler LC, et al. (2009) Cell shape changes indicate a role for extrinsic tensile forces in Drosophila germ-band extension. *Nat Cell Biol* 11(7):859–864.
6. Trepat X, Fredberg JJ (2011) Plithotaxis and emergent dynamics in collective cellular migration. *Trends Cell Biol* 21(11):638–646.
7. Razzell W, Wood W, Martin P (2014) Recapitulation of morphogenetic cell shape changes enables wound re-epithelialisation. *Development* 141(9):1814–1820.
8. Marinari E, et al. (2012) Live-cell delamination counterbalances epithelial growth to limit tissue overcrowding. *Nature* 484(7395):542–545.
9. Streichan SJ, Hoerner CR, Schneidt T, Holzer D, Hufnagel L (2014) Spatial constraints control cell proliferation in tissues. *Proc Natl Acad Sci USA* 111(15):5586–5591.
10. Mao Y, et al. (2011) Planar polarization of the atypical myosin Dachs orients cell divisions in Drosophila. *Genes Dev* 25(2):131–136.
11. Kondo T, Hayashi S (2013) Mitotic cell rounding accelerates epithelial invagination. *Nature* 494(7435):125–129.
12. Legoff L, Rouault H, Lecuit T (2013) A global pattern of mechanical stress polarizes cell divisions and cell shape in the growing Drosophila wing disc. *Development* 140(19):4051–4059.
13. Gibson MC, Patel AB, Nagpal R, Perrimon N (2006) The emergence of geometric order in proliferating metazoan epithelia. *Nature* 442(7106):1038–1041.
14. Hertwig O (1893) Ueber den Werth der ersten Furchungszellen für die Organbildung des Embryo. Experimentelle Studien am Frosch- und Tritonei. *Archiv für mikroskopische Anatomie* 42(4):662–807. German.
15. Minc N, Burgess D, Chang F (2011) Influence of cell geometry on division-plane positioning. *Cell* 144(3):414–426.
16. Théry M, et al. (2005) The extracellular matrix guides the orientation of the cell division axis. *Nat Cell Biol* 7(10):947–953.
17. Fink J, et al. (2011) External forces control mitotic spindle positioning. *Nat Cell Biol* 13(7):771–778.
18. Luxenburg C, Pasolli HA, Williams SE, Fuchs E (2011) Developmental roles for Srf, cortical cytoskeleton and cell shape in epidermal spindle orientation. *Nat Cell Biol* 13(3):203–214.
19. Campinho P, et al. (2013) Tension-oriented cell divisions limit anisotropic tissue tension in epithelial spreading during zebrafish epiboly. *Nat Cell Biol* 15(12):1405–1414.
20. Harris AR, et al. (2012) Characterizing the mechanics of cultured cell monolayers. *Proc Natl Acad Sci USA* 109(41):16449–16454.
21. Harris AR, et al. (2013) Generating suspended cell monolayers for mechanobiological studies. *Nat Protoc* 8(12):2516–2530.
22. Reinsch S, Karsenti E (1994) Orientation of spindle axis and distribution of plasma membrane proteins during cell division in polarized MDCKII cells. *J Cell Biol* 126(6):1509–1526.
23. Kunda P, Baum B (2009) The actin cytoskeleton in spindle assembly and positioning. *Trends Cell Biol* 19(4):174–179.
24. Stewart MP, et al. (2011) Hydrostatic pressure and the actomyosin cortex drive mitotic cell rounding. *Nature* 469(7329):226–230.
25. Weaire D, Hutzler S (2001) *The Physics of Foams* (Oxford Univ Press, Oxford).
26. Ranft J, et al. (2010) Fluidization of tissues by cell division and apoptosis. *Proc Natl Acad Sci USA* 107(49):20863–20868.
27. da Silva SM, Vincent JP (2007) Oriented cell divisions in the extending germband of Drosophila. *Development* 134(17):3049–3054.
28. Green AA, Kennaway JR, Hanna AI, Bangham JA, Coen E (2010) Genetic control of organ shape and tissue polarity. *PLoS Biol* 8(11):e1000537.
29. Keller R (1987) Cell rearrangement in morphogenesis. *Zoolog Sci* 4(5):763–779.